The Journal of Experimental Biology 215, 2108-2116

doi:10.1242/jeb.067603

RESEARCH ARTICLE

Targeting a neuropeptide to discrete regions of the motor arborizations of a single neuron

Daniel Kueh and John A. Jellies*

Department of Biological Sciences, Western Michigan University, Kalamazoo, MI 49008, USA

*Author for correspondence (john.jellies@wmich.edu)

SUMMARY

The heart excitor (HE) motor neuron in the leech *Hirudo* releases acetylcholine (ACh) and a peptide, FMRFamide, to regulate the contractile activity of the heart tube and associated side vessels. Consistent with Dale's principle, it was assumed that both neurotransmitters were localized to all presynaptic varicosities. However, we found discrete peptide-positive and peptide-negative varicosities associated with particular sites of innervation on the heart tube. We produced dual-labeled HE neurons by pressure injecting Neurobiotin into single HE cell bodies and applied anti-FMRFamide antibodies on the same preparations. Consistent with initial expectations, peptide-labeled varicosities were numerous and widely distributed along the heart tube and at one of the three side vessels, the latero-abdominal vessel. Nevertheless, some Neurobiotin-labeled varicosities along the heart tube lacked peptide label entirely. Moreover, there were dense and distinct peptide-negative innervations at the valve junctions of the latero-dorsal and latero-lateral vessels at each segment. Nevertheless, the peptide label was found in HE axons and varicosities that projected distally along the side vessels. Therefore, the more proximal peptide-negative clusters cannot simply be the result of restricted transport or deficient staining of peptide. Rather, we infer that FMRFamide is transported to (or selectively excluded from) discrete locations and that ACh is present in varicosities that lacked peptide. Such targeting of neurotransmitters could be described using a discrete targeting model of synaptic transmission. Compared with Dale's principle, this model may provide a more complete perspective of chemical communication than previously understood.

Key words: *Hirudo*, invertebrate, leech, discrete targeting, heart tube, motor neuron, peptide, acetylcholine, FMRFamide, varicosities.

Received 2 November 2011; Accepted 22 February 2012

INTRODUCTION

The heart excitor (HE) neuron in medicinal leeches, *Hirudo* spp., is a motor neuron that directly innervates a well-defined target, the heart tube (Thompson and Stent, 1976a; Jellies et al., 1992; Maranto and Calabrese, 1984a). To innervate the heart tube, an HE neuron projects its axon through the anterior nerve root that is located ipsilaterally (Thompson and Stent, 1976a). As the axon exits the anterior root, it branches and elaborates extensively, forming multiple arborizations over the heart tube and associated side vessels, thereby generating an elaborate plexus that regulates the contractile activity of the heart tube (Thompson and Stent, 1976a; Jellies et al., 1992; Maranto and Calabrese, 1984a; Wenning et al., 2004b).

Given that immunocytochemistry has shown FMRFamide to be widely distributed along the heart tube (Kuhlman et al., 1985a) and that choline acetyltransferase (ChAT) and acetylcholinesterase (AChE) were present in significant amounts in HE neurons and heart tube, Kuhlman et al. (Kuhlman et al., 1985a; Kuhlman et al., 1985b) have proposed that each HE neuron co-releases FMRFamide and ACh. Their suggestion is consistent with electron micrographs obtained by Maranto and Calabrese (Maranto and Calabrese, 1984a), which showed presynaptic terminals of HE neurons along the muscle of the heart tube that contain clear and dense core vesicles, and which presumably store ACh and FMRFamide neurotransmitters, respectively. Consistent with Dale's principle, it appeared that both ACh and FMRFamide would be co-released by each HE neuron at all target areas along the heart tube (Dale, 1935; Maranto and Calabrese, 1984a). Both ACh and FMRFamide have been found to increase the contractility of heart muscle cells as well as the strength of heart tube contractions (Calabrese and Maranto, 1986; Kuhlman et al., 1985b).

At each segment of each heart tube, three side vessels branch out to allow blood to circulate between the heart tube and body wall. Of these three side vessels, the latero-abdominal vessel (LaV) contains a sphincter and serves as an efferent vessel. Unlike the LaV, the latero-dorsal vessel (LdV) and the latero-lateral vessel (LlV) contain valves and serve as afferent vessels to receive blood from capillaries and body wall muscles (Boroffka and Hamp, 1969; Hammerson et al., 1976; Hildebrandt, 1988; Wenning et al., 2004a; Wenning and Meyer, 2007). Although innervation of the heart tubes has been studied extensively (e.g. Jellies et al., 1992; Thompson and Stent, 1976a; Thompson and Stent, 1976b; Thompson and Stent, 1976c; Maranto and Calabrese, 1984a; Maranto and Calabrese, 1984b; Wenning et al., 2004a), little is known about the innervation of the three side vessels, particularly at the junctions of these vessels. For example, Hammersen et al. (Hammersen et al., 1976) reported that muscle cells in the heart tube that are close to the valve junction regions receive innervation from a single type of axon that contained 'chiefly small, translucent vesicles', which differs significantly from the dual vesicle terminals belonging to HE neurons reported by Maranto and Calabrese (Maranto and Calabrese, 1984a) along the heart tube. Because Hammersen et al. (Hammersen et al., 1976) did not uniquely label individual neurons, they could not identify the source of these junctional terminals at that time.

To characterize the innervation of the three side vessel junctions at each segment of each heart tube, we produced dual-labeled HE neurons by pressure injecting Neurobiotin into individual HE cell bodies and applied anti-FMRFamide antibodies on the same preparations. As with the body of the heart tube, we found that the LaV sphincter and valve junctions of the LdV and LlV also received innervation from HE neurons. We also found that there were discrete peptide-positive and peptide-negative varicosities, which were consistently associated with particular sites of innervation on the heart tube. The consistency by which peptide-positive and peptide-negative varicosities appeared at the three side vessels led us to infer that an HE neuron does not release the same neurotransmitters at all of its target sites. Instead, each HE neuron selectively targets both neurotransmitters to areas along the heart tube and lateral vessels while specifically excluding one transmitter from the valve junction areas. These results provide further insights into the way an HE neuron discretely innervates each side vessel to regulate the contractions of those three vessels in conjunction with the heart tube, and suggest that the role of this single efferent neuron may be more elaborate than previously described.

MATERIALS AND METHODS

Preparations

Medicinal leeches, *Hirudo* spp. Linnaeus 1758, originally obtained from Leeches USA (Westbury, NY, USA) and Niagara Leeches (Cheyenne, WY, USA), were maintained in a breeding colony at room temperature (20°C). Animals were released from their cocoons at ≥30 days and were kept in 60×15 mm Petri dishes filled with 0.05% (w/v) artificial pond water [0.05% (w/v) Instant Ocean sea salt diluted in spring water; Spectrum Brands Inc., Madison, WI, USA]. The animals weighed between 29 and 40 mg. Only unfed animals at 30–90 days of age were used in this study as background autofluorescence from muscle and other tissues were more intense in large animals.

To prepare an animal for dissection, it was first anesthetized in a Sylgard-coated 60×15 mm dish that contained 5% ethanol-Ringer's solution. The leech Ringer's solution contained (in mmol l^{-1}) 115 NaCl, 4 KCl, 1.8 $CaCl_2$, 1.5 $MgCl_2$, 10 D-glucose, 4.6 Tris maleate and 5.4 Tris base, pH 7.4 (Nicholls and Baylor, 1968). Both suckers of each anesthetized animal, with its dorsal side up, were pinned to the dish with pins made from 0.05 mm tungsten wire (California Fine Wire Company, Grover Beach, CA, USA). An almost full-length incision was then made through the animal's dorsal skin, which allowed us to pin its body wall and to remove its crop, intestine and diverticula. Another incision was then made through the dorsal side of the ventral sinus that encased the midbody ganglia. The animal was then re-pinned with its ventral side up. Starting from midbody ganglia segment 3 (M3), seven incisions were made on the ventral side of the animal, with each incision exposing two midbody ganglia. The ventral side of the ventral sinus was also cut to fully expose each ganglion. Four additional pins were placed through the ventral skin around each ganglion to minimize muscle movements. The preparation was then rinsed with leech Ringer's solution and was allowed 5–10 min to recover.

Intracellular dye fills

To characterize innervation of the heart tube, we attempted to intracellularly inject up to 28 HE cell bodies from 14 midbody ganglia segments (M3–M16) in each of the eight animals with Neurobiotin (Vector Laboratories, Inc., Burlingame, CA, USA). Neurobiotin was diluted to 5% (w/v) with 0.25% (w/v) Fast Green FCF (Sigma-Aldrich, St Louis, MO, USA). Intracellular electrodes were fabricated from thin-wall capillary glass (o.d. 1 mm, i.d. 0.75 mm; World Precision Instruments, Sarasota, FL, USA) pulled on a Sutter P-87 puller (Sutter Instrument Company, Novato, CA, USA). Tips were backfilled with Neurobiotin by capillary action.

Once filled with Neurobiotin, the back end of each electrode was attached to a vinyl tube (i.d. 1 mm, o.d. 2 mm) connected to a 60 ml syringe, which allowed us to apply negative pressure to remove air bubbles from the tip of each electrode. To prevent clogging of the tip due to the drying out of Neurobiotin and Fast Green FCF, the electrodes were placed in a sealed container with a damp tissue for at least 2 h (4°C) before being used. Electrodes were then backfilled with 3 mol l^{-1} KCl. To slow down the rate of dilution of Neurobiotin, an air space between the KCl and Neurobiotin solutions was left close to the tip. Once an electrode was immersed in Ringer's solution, its tip was broken by gently pressing it against a pin to reduce the resistance of the electrode from >200 MΩ to approximately 80–90 MΩ. Intracellular dye injection into an HE cell body was completed using pressure (14–21 kPa) at 1 pulse s^{-1}. Reduction of spontaneous activity, hyperpolarized membrane potentials and presence of Fast Green FCF within a cell body were used as initial indications for the presence of Neurobiotin within each cell.

After filling, the preparation was re-pinned in a Sylgard-coated 35×10 mm Petri dish filled with an L-15 culture medium that contained (in final concentrations) 75% (v/v) Leibovitz L-15 culture medium, 25% (v/v) leech Ringer's solution and 6 mg ml^{-1} glucose. The culture medium was sterile filtered with a 0.2 μm filter. The preparation was then placed in a cold room (15°C) for 8 h to allow Neurobiotin to diffuse towards the periphery. The preparation was then fixed in a 4% (w/v) paraformaldehyde (PFA) fixative for another 8 h at 4°C. The tissue was then rinsed three times with phosphate buffered saline (PBS). Layers of unwanted tissues such as the dorsoventral muscles and nephridia were carefully removed to allow for better visualization of axons from HE neurons and to minimize background fluorescence.

Dye markers

To double label HE neurons, the preparations were first incubated with a primary rabbit anti-FMRFamide polyclonal antibody (Millipore, Billerica, MA, USA) and placed underneath an ice pack enclosed within a Styrofoam box on an orbital shaker (8 h). The primary antibody was diluted at 1:500 in a PBS-based vehicle that contained 1% Triton-X 100 with 0.1% NaN_3 and 10% goat serum. The tissue was then rinsed three times (30 min per rinse) with PBS before being treated with NeutrAvidin-Texas Red (Invitrogen, Carlsbad, CA, USA) and Alexa Fluor 488 conjugated to a goat-anti-rabbit antibody (Invitrogen) for another 8 h. Both markers were also diluted at 1:500 in vehicle. The preparation was then rinsed three times with PBS (30 min per rinse) before being dehydrated in a standard ethanol series (50–100%). It was cleared with methyl salicylate and mounted on a glass slide with DPX mounting medium (Electron Microscopy Sciences, Hatfield, PA, USA). To label only Neurobiotin or anti-FMRFamide, the above steps were repeated without the other fluorophore marker.

All whole mounts were examined with a Nikon EFD-3 epifluorescence microscope (Nikon Inc., Melville, NY, USA) equipped with a Kodak DC290 digital camera (Kodak, Rochester, NY, USA). Texas Red and Alexa Fluor 488 labeling were observed with excitation filters of 540–580 nm and 465–495 nm, respectively. Multiple pairs of digital fluorescent images of axons labeled by Neurobiotin and anti-FMRFamide were taken with Adobe

Photoshop CS 5 (Adobe Systems Inc., San Jose, CA, USA). To determine the depth of varicosities within the lumen of each side vessel, a subset of whole mounts were also examined with a Zeiss Axiovert 100 M confocal laser-scanning microscope (Carl Zeiss Microscopy, LLC, Thornwood, NY, USA). All *z*-stack images (0.86 μm per section) were taken under a 63× objective (C-Apochromat 63×/1.2 W Corr) and analyzed with an LSM 510 (Carl Zeiss Microscopy).

Histology

Two procedures were used to stain the heart tubes. In the first procedure, we applied 1% (w/v) Methylene Blue (dissolved in leech Ringer's solution), a stain that labels cell bodies (Macagno, 1980), on a subset of preparations. The preparations were then viewed under a dissecting microscope (World Precision Instruments) equipped with a digital camera. Images of the heart tubes were viewed and stored with IC Capture 2.1 (The Imaging Source, Charlotte, NC, USA). In another subset of preparations, a modified method by Karnovsky and Roots (Karnovsky and Roots, 1964) was used to stain the heart tubes for AChE (Karnovsky and Roots, 1964; Wallace and Gillon, 1982). Before staining, preparations were re-pinned with dried cactus spines, as the staining compounds would oxidize the tungsten wire pins. Tissues were fixed with 4% PFA (overnight at 4°C), rinsed with 0.1 mol l^{-1} sodium hydrogen maleate buffer, pH 6 (5 min), and incubated (1–2 h at 4°C) in a solution that contained (in final concentrations) 175 mmol l^{-1} sucrose, 0.5% (w/v) Triton X-100, 32.5 mmol l^{-1} sodium maleate, 5 mmol l^{-1} sodium citrate, 0.5 mmol l^{-1} potassium ferricyanide, 3 mmol l^{-1} cupric sulfate and 0.1 mg ml^{-1} acetylthiocholine iodide. Tissues were then placed in an ice-pack-filled Styrofoam box that sat on top of an orbital shaker for 8 h. Finally, tissues were rinsed three times with PBS, dehydrated using a standard ethanol series, cleared with methyl salicylate and mounted on glass slides with DPX mounting medium.

Data analysis

To count the arborizations and varicosities at each side vessel, we first took multiple pairs (Neurobiotin- and anti-FMRFamide-labeled axons) of fluorescent images from each preparation. To better visualize labeled varicosities and axons, we converted each image to black and white and made broad adjustments to its brightness and contrast using Adobe Photoshop CS 5. We then counted branch points and varicosities from each pair (Neurobiotin and anti-FMRFamide) of images. These varicosities and branch points were easily identifiable and were counted with the aid of the count tool in Adobe Photoshop CS 5. Branch points and varicosities were counted if they were located within the diameter of a side vessel and within 20 μm of the junction of the heart tube and side vessel. When branch points were counted, no distinctions were made between primary and secondary branch points. Branches that gave rise to three or more branches instead of just two branches were still counted as one branch point. Varicosities were counted if they were attached to a labeled axon.

All statistical analyses on the number of branch points and varicosities at each side vessel were based on the average number of branch points and varicosities from each preparation. To determine the ratio of anti-FMRFamide branch points to Neurobiotin branch points, we divided the average number of anti-FMRFamide branch points by the average number of Neurobiotin-labeled branch points from each animal. This approach was repeated with Neurobiotin- and anti-FMRFamide-labeled varicosities as well. All data were analyzed using two-way repeated-measures ANOVA, with the two factors being vessel type and dye label/tissue structures. A Tukey's test was conducted whenever significant results were found. Statistical significance was defined as $P<0.05$ for all tests. All graphs were plotted with GraphPad Prism 5 (GraphPad Software, Inc., La Jolla, CA, USA) and all statistical analyses were performed using SigmaPlot 10 (Systat Software, Inc., Point Richmond, CA, USA).

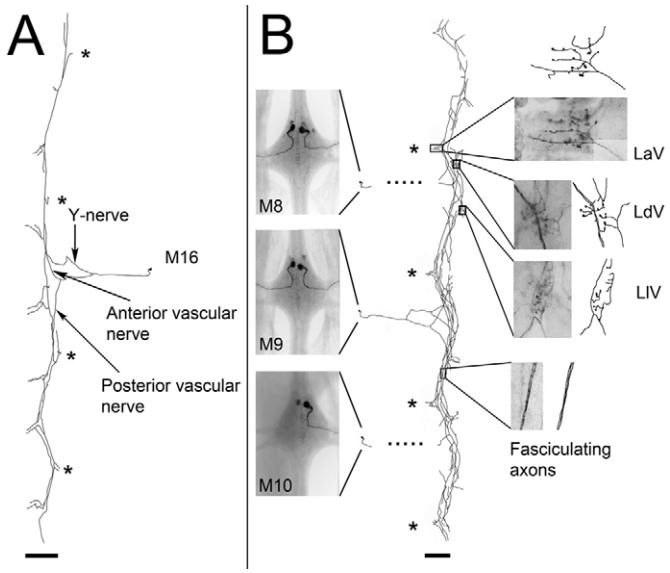

Fig. 1. Innervation of the heart tube of *Hirudo* sp. by three segmental heart excitor (HE) neuron homologs. Two-dimensional reconstructions were made of Neurobiotin-labeled HE neurons in (A) the left side of midbody ganglia segment 16 [M16(L)] and (B) M8–M10(R). Notable areas with fasciculated axons as well as varicosities present [latero-abdominal vessel (LaV) sphincter, and valve junctions of the latero-dorsal (LdV) and latero-lateral vessels (LlV)] were magnified and accompanied by corresponding traces. Scale bars, 1 mm. Asterisks mark the locations of the LaV vessels and dotted lines represent undrawn connections between HE neurons in M8 and M10 to their respective axons on the heart tube.

RESULTS

Innervation of the heart tube by HE neurons

Initially, we were interested in the specific target areas on the heart tube that were innervated by HE neurons. Based on previous studies (e.g. Jellies et al., 1992; Jellies and Kopp, 1995) as well as preliminary observations, we noticed that each Neurobiotin-labeled HE neuron extends over three to four segments of a heart tube (Fig. 1A). To determine the extent of overlap between three HE segmental homologs, we labeled HE neurons in three consecutive midbody ganglia segments (M8–M10) from one preparation by intracellularly injecting Neurobiotin into each HE cell body. Once Neurobiotin was coupled to NeutrAvadin-Texas Red, we were able to identify HE neurons at each midbody ganglion based on the placement of their cell bodies (e.g. Fig. 1B) and the ipsilateral direction by which they exit through their respective midbody ganglia (Thompson and Stent, 1976a; Jellies and Kopp, 1995). Dye diffusion of Neurobiotin allowed us to follow the axon of each HE neuron through the anterior nerve root located on the ipsilateral side of each midbody ganglion. Multiple exemplary images were taken and were assembled into a collage, which was then reconstructed as a two-dimensional black and white outline of these of images (Fig. 1).

As we examined the axons of the three HE neurons that traverse to and along the heart tube, we found that the pattern of innervation

by each cell was consistent from one midbody segment to the next. For example, when the axon of an HE neuron from the right side of the ninth midbody segment [M9(R)] reached the heart tube within the same segment, its axon bifurcated to innervate the heart tube approximately one segment anterior and one segment posterior (Fig. 1B). Bifurcations resulting in Y-nerves as well as anterior and posterior vascular nerves were also observed in segmental HE homologs at M8(R) and M10(R) (not shown). As a result, the axons from the three ipsilateral HE segmental homologs fasciculated to provide continuous and overlapping innervation along the heart tube.

Consistent with previous studies by Kuhlman et al. (Kuhlman et al., 1985a), we were able to identify Neurobiotin-labeled axons belonging to HE neurons that extend along the heart tube (Fig. 1). Moreover, we also found Neurobiotin-labeled varicosities at all three associated side vessels: LaV, LdV and LlV (Fig. 1B). The varicosities at the LaV often appeared in linear series with each other on each axon. Unlike the junction of the LaV, the presence of Neurobiotin-labeled varicosities belonging to HE neurons at the junctions of the LdV and the LlV was unexpected (Fig. 1B) because the varicosities at the junctions of these two afferent side vessels have not previously been revealed when preparations were immunolabeled with an antibody against FMRFamide. The varicosities at the junctions of these two side vessels were often grouped together as dense clusters of varicosities, with each cluster branching off from an axon at the corner of the junction of each vessel (Fig. 1B). When focusing through the specimen, these clusters appear to be within the valve junctions of these two side vessels (Fig. 1B). Furthermore, the clusters of varicosities at each side vessel junction may belong to at least three segmental HE homologs because there is extensive overlap between the HE axons at M8–M10 (Fig. 1B). Finally, because these clusters of varicosities could not be revealed with immunolabeling, but only with intracellular injections of Neurobiotin, we hypothesized that HE neurons may discretely target peptide and non-peptide-containing varicosities to specific target sites on the heart tube.

Double labeling of HE axons on the heart tube and LaV

To examine our hypothesis that there was discrete targeting of peptide and non-peptide varicosities at specific target sites on the heart tube, we used a double label technique to determine whether axons from HE neurons labeled with Neurobiotin coupled to NeutrAvidin-Texas Red would also be identifiable with an anti-FMRFamide antibody coupled to an Alexa-Fluor-488-tagged secondary antibody. Of the possible total of 224 HE neurons from eight preparations (28 cells per preparation) that we attempted to label with Neurobiotin, 141 HE neurons (63.0±6.0%) were successfully labeled (Table 1). We took a pair (Neurobiotin- and anti-FMRFamide-labeled axons) of exemplary images from the LaV, LlV and LdV. With respect to the total number of images taken from these eight preparations, there were 53 pairs of images taken from the LaV, 56 pairs from the LlV and 37 pairs from the LdV.

As before, we followed the Neurobiotin-labeled axons of HE neurons as they reached and aligned along a heart tube (Fig. 2A). The labeled axons of three consecutive HE segmental homologs overlapped in all of the preparations. Axons that were labeled by Neurobiotin (red) were also identifiable with the anti-FMRFamide label (green) (Fig. 3B). When we merged the two different fluorescent images of the same axons, we found that the two fluorescent labels colocalized completely with each other (Fig. 2C). Both labels also allowed us to follow these axons to the LaV, where the fibers would sprout to form varicosities that terminated close to the junction of the LaV. As with the double labeling of HE axons on the heart tube, there was almost complete colocalization of both labels at the LaV (Fig. 2C).

Table 1. Number of heart excitor neurons in each preparation that were labeled with Neurobiotin

Preparation	Left	Right	Total	% Filled
1	8	10	18	64.3
2	9	10	19	67.9
3	9	9	18	64.3
4	5	7	12	42.9
5	13	11	24	85.7
6	6	7	13	46.2
7	11	13	24	85.7
8	6	7	13	46.4
Mean ± s.e.m.	8.4±0.58	9.5±0.52	17.7±0.77	63.0±6.0
Total	67	74	141	–

Rarely, we found a Neurobiotin-labeled axon that did not colocalize completely with anti-FMRFamide. For example, we found axons or varicosities that were revealed by the anti-FMRFamide label but not with the Neurobiotin label. However, these examples represented a small fraction of the total label along the heart tube and LaV, which we attributed to a lack of diffusion of Neurobiotin. In other instances, the Neurobiotin label would reveal clusters of varicosities that branched from an HE axon on the heart tube but were not revealed by the anti-FMRFamide label (Fig. 3A). Such clusters, although rarely seen along the heart tube, indicated that colocalization of the two fluorescent labels was not always complete (Fig. 3C). Likewise, similar instances were also observed at the sphincter area of the LaV, whereby occasional varicosities were revealed by the Neurobiotin label (Fig. 3D) but not with the anti-FMRFamide label (Fig. 3E). When certain parts of an axon or attached varicosities were revealed by Neurobiotin but not by the anti-FMRFamide label, these parts were inferred to be peptide-negative (Fig. 3F).

Neurobiotin-labeled varicosities at the LdV and LlV were mainly peptide-negative

If our hypothesis of HE neurons being able to discretely target peptide and non-peptide varicosities was correct, we predicted that most peptide-positive varicosities at the LaV junction and heart tube would be visible with both Neurobiotin (red) and anti-FMRFamide (green) whereas peptide-negative varicosities at select and discrete locations such as the LdV and LlV junctions would only be visible with Neurobiotin. This would be consistent with our preliminary observations of Neurobiotin-labeled varicosities being present at the junctions of the LdV and LlV (Fig. 1B). Our results supported this prediction as we followed the Neurobiotin-labeled axons to the LdV and LlV (Fig. 4A,D). We consistently observed clusters of varicosities at the valve junctions of these two side vessels, as previously revealed by Neurobiotin alone, but these clusters were not visible with the anti-FMRFamide label (Fig. 4B,E). However, HE axons that projected distally along the side vessels could be visualized with both the Neurobiotin and anti-FMRFamide labels. In summary, there appears to be little to no colocalization between the two dye markers at the valve junctions of the LdV and LlV, which we observed repeatedly in multiple segments and in all preparations.

To determine the depth of Neurobiotin-labeled varicosities at the junctions of the three side vessels, we used confocal laser-scanning microscopy to construct multiple *z*-stack images of all three side vessels at an interval of 0.84–0.86 μm. In the LaV, clusters of

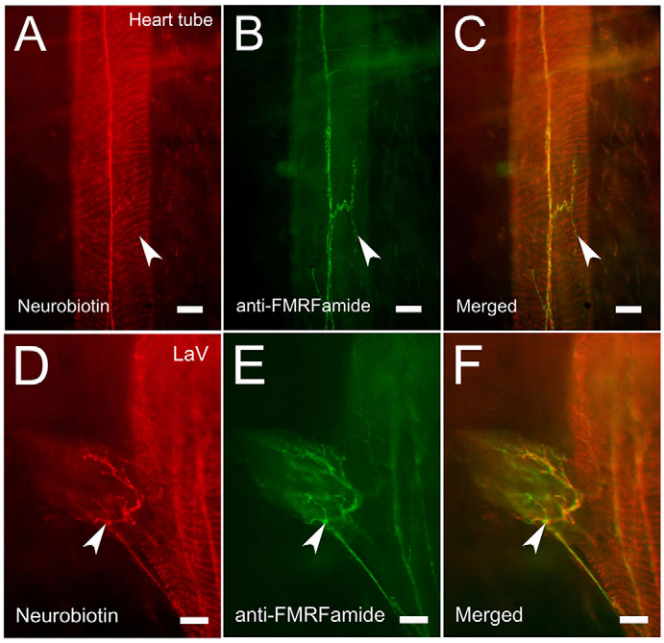

Fig. 2. Double labeling of the heart tube and LaV of *Hirudo* sp. (A–C) Axons on the heart tube at M4(R) and (D–F) varicosities at the LaV at M9(R) were labeled by (A,D) Neurobiotin conjugated to NeutrAvidin-Texas Red (red) and (B,E) anti-FMRFamide conjugated to an Alexa-Fluor-488-tagged secondary antibody (green). (C,F) Merging of images shows colocalization (yellow). A small number of anti-FMRFamide-labeled varicosities did not completely colocalize with Neurobiotin-labeled varicosities. Arrowheads point to clusters of varicosities. Scale bars, 20 μm.

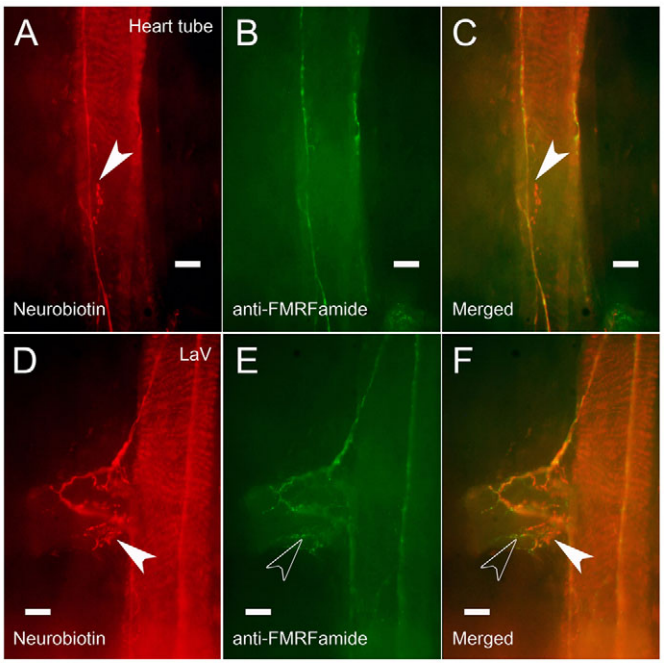

Fig. 3. Certain axons and varicosities on the heart tube and LaV of *Hirudo* sp. could only be visualized with one of the two dye markers. A cluster of varicosities on the heart tube at M8(L) can be observed with (A) the Neurobiotin label but not with (B) the anti-FMRFamide label. (C) A merged image of both fluorophore markers revealed varicosities that were labeled with just one of the two labels. Clusters of varicosities from the junction to the sphincter area of the LaV at M7(L) can be observed when labeled with (D) Neurobiotin, but not with (E) anti-FMRFamide. (F) A merged image of both fluorophore markers revealed varicosities around the sphincter area of the LaV that were labeled with just one of the two labels. The anti-FMRFamide-labeled varicosities deep within the vessel were not labeled with Neurobiotin because of a lack of diffusion by Neurobiotin towards the deeper ends of the vessel. Filled arrowheads point to Neurobiotin-labeled varicosities whereas unfilled arrowheads point to a cluster of FMRFamide-labeled varicosities. Scale bars, 20 μm.

varicosities can be found on the dorsal (Fig. 5A) and ventral (Fig. 5C) surfaces as well as along the vessel and muscle sphincter (Fig. 5B). At the valve junctions of the LdV and LlV, however, the large clusters of peptide-negative varicosities could only be seen beneath the most superficial muscle layers. For example, in one preparation, large clusters of Neurobiotin-labeled varicosities (Fig. 5E) started to appear ~6 μm from the dorsal surface (Fig. 5D) and ~4.2 μm from the ventral surface (Fig. 5F) of the LdV junction at M3(R). In that same preparation, large clusters of Neurobiotin-labeled varicosities (Fig. 5H) started to appear ~15 μm away from the dorsal surface (Fig. 5G) and ~8.4 μm away from the ventral surface (Fig. 5I) of the LlV junction at M6(R). Thus, innervation of each LdV or LlV junction appears to be heavily concentrated within the valve junction itself.

Once we identified the locations that contained large clusters of labeled varicosities, we counted the number of branch points (see Fig. 6A) at the three side vessels and found that the number of branch points were dependent upon the type of side vessel to which they were targeted ($F_{2,12}$=19.2, P<0.001; Fig. 6B). Specifically, significantly fewer branch points were found at the LdV and LlV than at the LaV (Tukey's test, all P<0.001). When we compared double-labeled branch points within a side vessel, we found no significant differences between the mean (±s.e.m.) number of Neurobiotin- and anti-FMRFamide-labeled varicosities at the LaV (Fig. 6B). Neurobiotin was therefore able to diffuse past second- and third-order branchings at the LaV. At the LdV, however, there was a mean of 4.4±0.7 Neurobiotin-labeled branch points (range 2.7–8.2, N=8), which was significantly greater than the mean of 1.5±0.2 anti-FMRFamide-labeled branch points (range 0.8–2.3, N=8; Tukey's test, P<0.001; Fig. 6B). Likewise, there was a mean of 4.0±0.7 Neurobiotin-labeled branch points (range 2.4–7.3, N=7) at the LlV, which was also significantly greater than the mean of 1.2±0.4 anti-FMRFamide-labeled branch points (range 0–2.7, N=7) within the same vessel (Tukey's test, P<0.001; Fig. 6B). Thus, there appears to be little colocalization between the two labels with respect to the branch points at the junctions of the LdV and LlV.

As we counted varicosities (see Fig. 6A) at the neuronal branches that terminated at the three side vessels, we found significant differences between the Neurobiotin-labeled varicosities and anti-FMRFamide-labeled varicosities at each of the three side vessels ($F_{1,6}$=13, P=0.011; Fig. 6C). At the LaV, there was a significant difference between the mean of 28.1±5 (range 13.5–50.2, N=8) varicosities labeled by Neurobiotin and the mean of 43.1±7 varicosities (range 16.3–72.3, N=8) labeled by anti-FMRFamide (Tukey's test, P<0.001). At the other two side vessels, however, the differences were reversed. For example, at the LdV, there was a mean of 19.6±2.7 (range 10–33, N=8) varicosities labeled by Neurobiotin, which significantly outnumbered the mean of 6.7±1.4 (range 2.2–15, N=8) varicosities labeled by anti-FMRFamide (Tukey's test, P<0.001). Similarly, at the LlV, the mean of 16.7±2.8 (range 5.5–26.3, N=7)

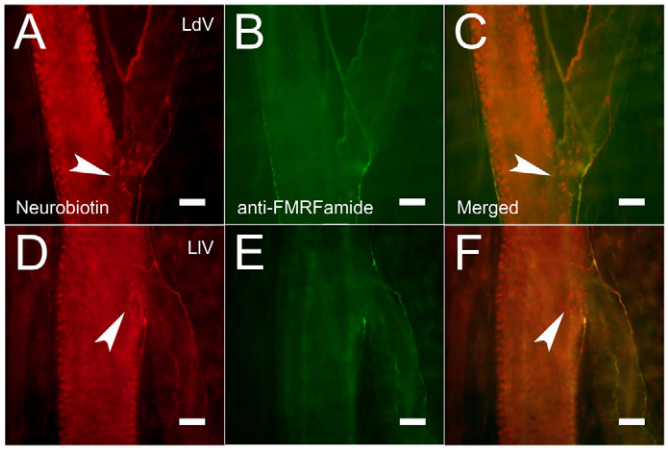

Fig. 4. Varicosities at the valve junctions of the LdV and LIV in *Hirudo* sp. were not labeled with anti-FMRFamide. Clusters of varicosities at the valve junctions of the (A) LdV and (D) LIV at M6(R) were clearly visible when labeled with Neurobiotin, but were conspicuously absent when labeled with (B,E) anti-FMRFamide. Overlaid images revealed varicosities at the valve junctions of the (C) LdV and (F) LIV that were labeled with Neurobiotin but not with the anti-FMRFamide. Arrowheads point to Neurobiotin-labeled varicosities. Scale bars, 20 μm.

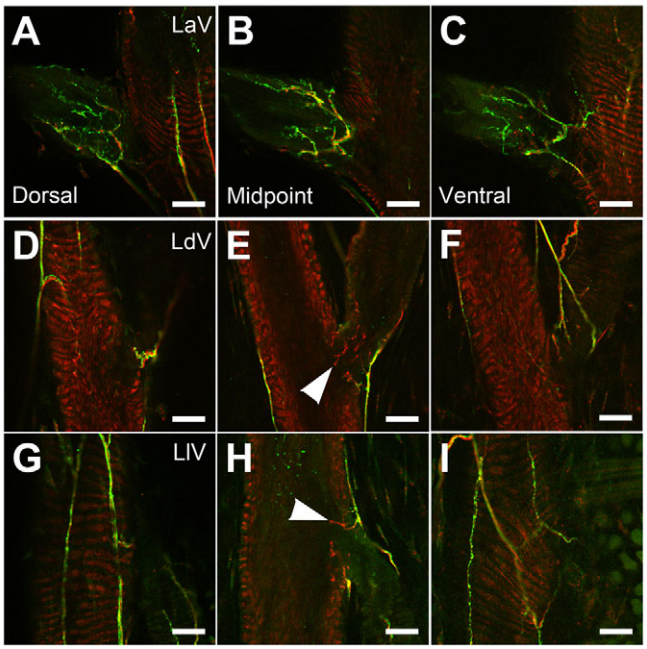

Fig. 5. Confocal micrographs of the three side vessels of *Hirudo* sp. at different depths of focus. (A–C) The same LaV shown in Fig. 2D,E. (D–F) The same LdV shown in Fig. 4A–C. (G–I) The same LIV shown in Fig. 4D–F. At the LaV, large clusters of varicosities are visible on the (A) dorsal and (C) ventral surfaces as well within the (B) sphincter junction of the vessel. In contrast, large clusters of peptide-negative varicosities are not visible at the (D,G) dorsal or (F,I) ventral surfaces of the LdV and LIV junctions at M6(R). Instead, they were only visible deep within the (E,H) valve junctions of the two side vessels. Arrowheads point to Neurobiotin-labeled varicosities. Scale bars, 20 μm.

varicosities labeled by Neurobiotin significantly outnumbered the mean of 5±1.7 (range 0–13, N=7) varicosities labeled by anti-FMRFamide (Tukey's test, P<0.001).

When we expressed the number of branch points at the three side vessels as a ratio of anti-FMRFamide-labeled branch points over Neurobiotin-labeled branch points, we were able to infer the extent to which Neurobiotin-labeled branches colocalized with anti-FMRFamide-labeled branches. Three inferences can be made with respect to the mean ± s.e.m. ratio of double-labeled branches. First, a ratio of 1 indicates a 100% colocalization between the two fluorescent dyes. Second, a ratio of >1 would indicate that there were more branch points labeled with anti-FMRFamide and fewer branch points labeled with Neurobiotin. Had there been equal number of branch points labeled with both Neurobiotin and anti-FMRFamide, then colocalization would have been 100%. Finally, a ratio of <1 would indicates that <100% of the Neurobiotin-labeled branches were labeled with anti-FMRFamide, which we would therefore classify as peptide-negative. Ratio measurements were applied to Neurobiotin- and anti-FMRFamide labeled varicosities as well.

As expected, we found the proportion of colocalization between Neurobiotin- and anti-FMRFamide-labeled branch points and varicosities to be dependent upon the type of side vessel ($F_{2,12}$=39.2, P<0.001; Fig. 6D). Specifically, colocalizations were significantly greater at the LaV than at the LdV and LIV (Tukey's test, all P<0.001). Significant differences were found between the mean ratio of 1.2±0.1 branch points and the mean ratio of 1.7±0.2 varicosities at the LaV (Tukey's test, P=0.003). No significant differences were found between the branch points and varicosities at the LdV and LIV. Based on the lack of colocalization at the two afferent vessels, we concluded that varicosities at the LdV and LIV were mainly peptide-negative, resulting from the peptide not being transported pass the second- and third-order branches towards the varicosities, despite the ability of HE neurons to transport peptides to more distal locations along the muscles of the two afferent vessels.

Side vessel junctions and AChE activity

Because we found significant numbers of Neurobiotin-labeled varicosities that were devoid of peptide at the valve junctions of the LdV and LIV, we were interested in the general morphological characteristics of the LdV and LIV junctions in comparison to the LaV and the rest of the heart tube. In a group of preparations that were stained with Methylene Blue, staining was most intense at the heart tube and LaV sphincters as well as at the LdV and LIV junctions (Fig. 7A). Consistent with previous studies (e.g. Maranto and Calabrese, 1984a; Hildebrandt, 1988; Hammersen et al., 1976), the density and type of cells at these areas appear to be different from those that make up the rest of the heart tube.

Given that nicotinic acetylcholine receptors in the leech are unresponsive to α-bungarotoxin (Calabrese and Maranto, 1986), it is difficult to determine directly the relative distribution of cholinergic receptors in the heart tube and side vessels. As it is still possible to stain for AChE, we wanted to determine whether staining of AChE activity at the three side vessels was similar to each other and to the rest of the heart tube. We found that the LdV and LIV junctions stained more heavily for AChE (Fig. 7C,D) whereas the intensity of the AChE activity at the LaV junction was similar to the rest of the heart tube. Nevertheless, the sphincter area of the LaV was stained a little more heavily than the rest of the heart tube (Fig. 7B), though apparently less than the valve junctions associated with afferent vessels using this histochemical procedure. Thus, although cholinergic activity can be found in all parts of the heart tube and associated side vessels as expected, it is particularly conspicuous at the LdV and LIV junctions and at the LaV sphincter.

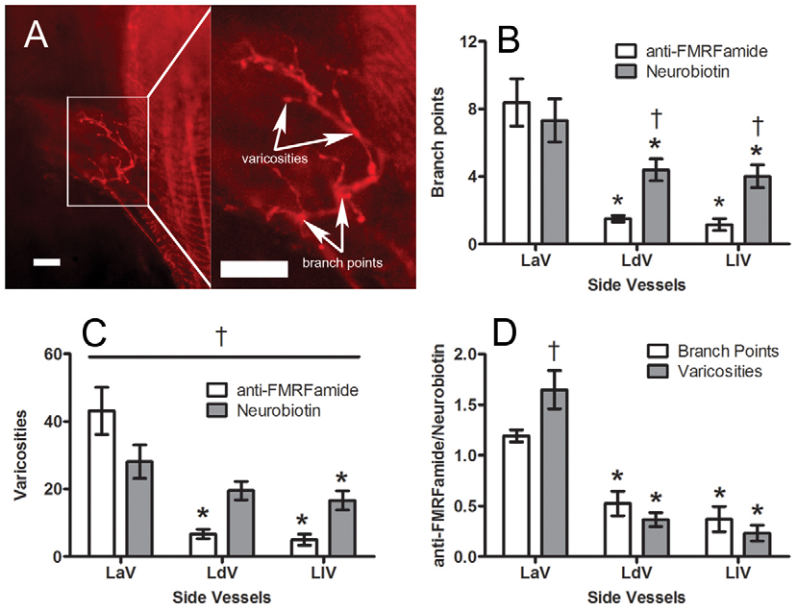

Fig. 6. Differences in the mean (±s.e.m.) number of labeled arborizations and varicosities at the junctions of the three side vessels of *Hirudo* sp. (A) Labeled branch points and varicosities such as those in LaV (same as Fig. 2D) were counted. Scale bars, 20 μm. Based on these counts, we found significant differences between the mean (±s.e.m.) numbers of Neurobiotin- and FMRFamide-labeled (B) branch points and (C) varicosities within the LdV (N=8) and LlV (N=7) and between the LaV (N=8) and the other two afferent vessels. (D) The mean (±s.e.m.) ratio of anti-FMRFamide- to Neurobiotin-labeled branch points and varicosities was significantly lower at the LdV and LlV relative to the LaV. Asterisks represent a significant difference from the LaV whereas daggers represent a significant difference between Neurobiotin and anti-FMRFamide or between varicosities and branch points (Tukey's test, P<0.05). Error bars represent ±s.e.m.

DISCUSSION

In the present study, we found that there is overlapping innervation between each HE neuron as axons from each cell spanned approximately three midbody segments in the periphery. We also found that in addition to innervating the heart tube, HE neurons also innervated the three associated side vessels at each segment of the heart tube. Finally, we found that varicosities at the LaV and along the heart tube were mainly peptide-positive, as expected, whereas HE varicosities at the LdV and LlV junctions were predominantly peptide-negative. These findings were consistently found in multiple midbody segments and in different animals.

Hildebrandt (Hildebrandt, 1988) suggested that neurons in the nerve cord might send out axons to innervate the three side vessels. We identified labeled axons belonging to HE neurons at the LaV sphincter and at the valve junctions of the LdV and LlV. Furthermore, we found that vessel type and location were the best predictors of the abundance of peptide-containing varicosities (Fig. 6B–D). This led us to consider the morphological and functional differences between the three side vessels. Based on the Methylene Blue staining of the heart tube (Fig. 7A), the tissue morphology that made up the side vessels is different from the rest of the heart tube. For example, the heart tube sphincter is made up primarily of *cis* muscle cells, which have extra longitudinal arms that thicken the sphincter walls of the heart tubes (Maranto and Calabrese, 1984a). Thus, Methylene Blue staining would be more pronounced in sphincter areas of the heart tube (Fig. 7A). With respect to the heavily stained valve junctions of the LdV and LlV, Hammersen et al. (Hammersen et al., 1976) observed these junctions to contain multiple finger-like projections or villi (Hammersen et al., 1976). Unlike the rest of the heart tube, these villi are made of specialized cells, perhaps of endothelial origin. Although it is not clear whether the development of peptide-negative varicosities is dependent on their presence, the valve junctions present a different tissue environment than the LaV sphincter or heart tube.

As the clusters of Neurobiotin-labeled varicosities that are peptide-negative were mainly found within the valve junctions of the LdV and LlV, it has not escaped our attention that such observations could, in principle, result from deficient staining of FMRFamide. There are three reasons why we suggest this is unlikely. First, anti-FMRFamide-labeled axons at the same focal plane were consistently present and projected distally along the two side vessels, which colocalized with distally projected Neurobiotin-labeled axons (Fig. 4). Moreover, some varicosities could be found at comparable depths within the LaV sphincter, an area surrounded by thicker tissues (Fig. 7A) that may be just as likely to prevent access as those that surround the valve junctions of the LdV and LlV. Second, the animals that were used in this study were unfed juveniles, relatively small in size. The tissues of these animals were less dense compared with those found in larger animals. The peptide-positive cells and processes widely found elsewhere in these animals

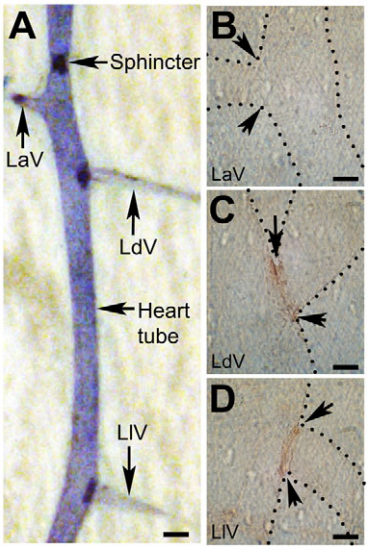

Fig. 7. Staining of the heart tube and side vessels of *Hirudo* sp. (A) A right heart tube from a fed animal that was stained with Methylene Blue. Scale bar, 1 mm. Anterior is upwards. Staining is noticeably intense at the LdV and LlV junctions as well as at the heart tube and LaV sphincter areas. The staining of AChE on the heart tube and side vessels was most noticeable at the (C,D) junctions of the LdV and LlV but not at the junction of the (B) LaV. Arrowheads in B–D point towards the junction of each side vessel. Scale bars, 20 μm.

could be labeled reliably with the peptide antibody deep within the midbody ganglia and body wall muscle. Third, because the Neurobiotin label was successfully visualized by application of a large, fluorescently tagged avidin that also had to have diffused through the region, it seems unlikely that the primary and secondary antibodies would have been uniquely excluded from just those regions.

The lack of FMRFamide-labeled arborizations and varicosities at the junctions of the LdV and LlV led us to infer that the transport of neuropeptides to the junctions of those two side vessels is somehow restricted by HE neurons. Such selective transport of neuropeptide by HE neurons would explain the apparent discrepancy between the ultrastructural images taken by Maranto and Calabrese (Maranto and Calabrese, 1984a) of HE terminals along the heart tube and those taken by Hammersen et al. (Hammersen et al., 1976) at the afferent valve-junction regions. When Maranto and Calabrese (Maranto and Calabrese, 1984a) obtained thin sections from an isolated heart tube, they found that the presynaptic terminals belonging to HE neurons appeared to contain both clear and dense core vesicles, which presumably store ACh and FMRFamide, respectively (Maranto and Calabrese, 1984a). We suggest that the ultrastructure of peptide-positive varicosities at the LaV would be identical or similar to the ones found along the heart tube as revealed by Maranto and Calabrese (Maranto and Calabrese, 1984a). In contrast to the findings of Maranto and Calabrese (Maranto and Calabrese, 1984a), Hammersen et al. (Hammersen et al., 1976) specifically noted that the terminal 'axons' at the valve junctions of afferent vessels contained clear vesicles, and in fact they did not include figures that showed any dense core vesicles. Although Hammersen et al. (Hammersen et al., 1976) did not identify the neurons that these axons belong to, our results strongly suggest that those axons with clear vesicles are the peptide-negative varicosities that belong to HE neurons. The suggestion that each HE neuron forms two morphologically distinct synapses is not entirely without precedent, as Hattori et al. (Hattori et al., 1991) found that individual dopaminergic neurons in the striatum of rat brains can form symmetric and asymmetric synapses.

As our results were based entirely on the presence and absence of FMRFamide immunolabeling, it is not clear whether there is discrete targeting of ACh at those three side vessels as well. Nevertheless, we found this to be unlikely as Neurobiotin-labeled varicosities were widely present at the junctions of the LdV and LlV (Fig. 4) as well as along the heart tube, side vessels and LaV sphincter. Based on the very heavy staining for AChE at those two side vessel junctions specifically, as well as the presence of clear vesicles in axons located at valve junction regions as revealed by Hammersen et al. (Hammersen et al., 1976), it is likely that the synapses at the LdV and LlV junctions are primarily cholinergic. Because acetylcholine binds with nicotinic acetylcholine receptors on the heart tube to generate ionotropic responses (Calabrese and Maranto, 1986), it is possible that direct application of curare may also inhibit the normal functioning of these two side vessels. It will be of interest in future studies to test the influence of activity of these regions on constriction patterns of the heart tube and side vessels.

During the Walter Ernest Memorial Lecture, Dale (Dale, 1935) suggested that the release of a known neurotransmitter by the presynaptic terminal of a neuron in the peripheral nervous system could provide an indication of the type of neurotransmitter that was released by another presynaptic terminal of that same neuron in the central nervous system. First defined by Eccles in 1952 and later formalized as a principle in 1976, Eccles defined Dale's principle to mean that each neuron would release the same group of neurotransmitters at all of its presynaptic terminals (Eccles et al., 1954; Eccles, 1976). However, the principle is sometimes interpreted to mean that one neuron would release only one type of neurotransmitter at all of its nerve terminals (Burnstock, 2006), which has been falsified repeatedly (e.g. Nusbaum et al., 2001; Vaney and Young, 1988).

The original definition of Dale's principle has been previously challenged by three key studies. In the first study, Sossin et al. (Sossin et al., 1990) used electron microscopic immunocytochemistry to show distinct classes of peptide-containing vesicles localized to separate presynaptic terminals belonging to the same bag cells in *Aplysia californica*. Their findings were consistent with a later study by Hattori et al. (Hattori et al., 1991), which found that individual dopaminergic neurons in the striatum of rat brains are able to form two types of synaptic contacts (symmetric and asymmetric) with other striatal cells. To visualize these synapses, Hattori et al. (Hattori et al., 1991) double labeled these dopaminergic neurons with an antibody against the dopamine-synthesizing enzyme tyrosine hydroxylase and an injection of a radioactive isotope, tritium (^{3}H), that was tagged to the amino acid leucine (^{3}H-leucine). They found that symmetric synapses formed by dopaminergic neurons could be immunolabeled, but not radiolabeled, whereas asymmetric synapses formed by these same neurons could be radiolabeled and immunolabeled (Hattori et al., 1991). Hattori et al. (Hattori et al., 1991) concluded that while both synapses probably belonged to the same neuron, only one of the synaptic contacts could be labeled with a dopaminergic marker. Thus, it appeared that a dopaminergic neuron was able to form dopaminergic and non-dopaminergic synapses. Finally, Sámano et al. (Sámano et al., 2006) used immunohistochemistry to show that ChAT colocalized with other neuropeptides such as methionine-enkephalin, somatostatin and neurotensin in cell bodies of sympathetic preganglionic neurons (SPNs) of cats. Such colocalization was largely absent in the axon fibers and presynaptic terminals of SPNs at the stellate ganglion and sympathetic thoracic trunk of the animal. Because immunolabeling for ChAT tends to match the immunolabeling of ACh in the central nervous system, Sámano et al. (Sámano et al., 2006) suggested that SPNs may synthesize ChAT and neuropeptides in their cell bodies but transport them separately to different locations.

Our study is consistent with the studies by Sossin et al. (Sossin et al., 1990), Hattori et al. (Hattori et al., 1991) and Sámano et al. (Sámano et al., 2006) in three respects. First, in all four studies, markers were used to identify the neurotransmitters of interests, and the absence or presence of these markers at a specific location was used to indicate the presence of a specific neurotransmitter of interest. Thus, reliability of these markers is crucial to conclusions about discrete targeting of neurotransmitters to specific areas. Second, the targeting of neurotransmitters by these different neurons appeared to be based on exclusion, as these neurons would target two neurotransmitters to one location while excluding one of the two neurotransmitters (usually a neuropeptide) from being released in another location. Finally, all four studies have provided exceptions to Dale's principle, whereby a single neuron would not necessarily target the same neurotransmitter to all target areas. Despite these similarities, the present study differs from the studies by Sossin et al. (Sossin et al., 1990), Hattori et al. (Hattori et al., 1991) and Sámano et al. (Sámano et al., 2006) as the observed mismatch in colocalization in the present study can be traced to a single identifiable neuron rather than a group of neurons, eliminating a source of ambiguity. Moreover, our study focuses on the peripheral

interaction between a motor neuron and an effector, specifically, the muscle cells at the junction of the side vessels rather than the interaction between two neurons. The discrete targeting of a neuropeptide by HE neurons may have direct functional implications with respect to the circulatory system in the medicinal leech, a system very amenable to detailed physiological analysis. Thus, it may be possible in future studies to directly test the functional implications of the discrete targeting of a neuropeptide, shown here by anatomical methods.

Based on the results from the present study, as well as the diversity of synaptic connections that an individual neuron can form with other cells, it appears that a model neuron based on Dale's principle would not be adequate when describing the formation and function of neuronal circuits. Thus, a better alternative might be a discrete targeting model of synaptic transmission, as originally suggested by Sossin et al. (Sossin et al., 1990). Such a model would have greater generality, as it does not necessarily assume that there will be differential allocation of different neurotransmitters to different locations. Rather, it would allow for such an assumption while not excluding the possibility of targeting neurotransmitters to discrete locations. Based on the discrete targeting model of synaptic transmission, we propose that the HE neuron releases ACh at all of its target sites while selectively targeting the release of FMRFamide to specific locations on the heart tube and excluding it from other focal peripheral sites.

LIST OF ABBREVIATIONS

ACh	acetylcholine
AChE	acetylcholinesterase
ChAT	choline acetyltransferase
HE	heart excitor
LaV	latero-abdominal vessel
LdV	latero-dorsal vessel
LlV	latero-lateral vessel
M	midbody ganglion
PBS	phosphate buffered saline
SPN	sympathetic preganglionic neuron

ACKNOWLEDGEMENTS

We would like to acknowledge the exceptional technical assistance of Christine Eskander in the preparation of AChE stained preparations.

FUNDING

This study was supported in part by the Gwen Frostic Award, the Patricia L. Thompson Dissertation Award (D.K.) and the Western Michigan University Faculty Research and Creative Activity Award (J.A.J.).

REFERENCES

Boroffka, I. and Hamp, R. (1969). Topographie des Kreislaufsystems und Zirkulation bei *Hirudo medicinalis*. *Zoomorphology* **64**, 59-76.

Burnstock, G. (2006). Historical review: ATP as a neurotransmitter. *Trends Pharmacol. Sci.* **27**, 166-176.

Calabrese, R. L. and Maranto, A. R. (1986). Cholinergic action on the heart of the leech, *Hirudo medicinalis*. *J. Exp. Biol.* **125**, 205-224.

Dale, H. (1935). Pharmacology and nerve-endings (Walter Ernest Dixon Memorial Lecture). *Proc. R. Soc. Med.* **28**, 319-332.

Eccles, J. (1976). From electrical to chemical transmission in the central nervous system. *Notes Rec. R. Soc. Lond.* **30**, 219-230.

Eccles, J., Fatt, P. and Koketsu, K. (1954). Cholinergic and inhibitory synapses in a pathway from motor-axon collaterals to motoneurones. *J. Physiol.* **126**, 524-562.

Hammersen, F., Staudte, H.-W. and Möhring, E. (1976). Studies of the fine structure of invertebrate blood vessels. II. The valves of the lateral sinus of the leech, *Hirudo medicinalis* L. *Cell Tissue Res.* **172**, 405-423.

Hattori, T., Takada, M., Morrizumi, T. and Van Der Kooy, D. (1991). Single dopaminergic nigrostriatal neurons form two chemically distinct synaptic sites: possible transmitter segregation within neurons. *J. Comp. Neurol.* **309**, 391-401.

Hildebrandt, J. (1988). Circulation in the leech, *Hirudo medicinalis* L. *J. Exp. Biol.* **134**, 235-246.

Jellies, J. and Kopp, D. M. (1995). Sprouting and connectivity of embryonic leech heart excitor (HE) motor neurons in the absence of their peripheral target. *Invertebr. Neurosci.* **1**, 145-157.

Jellies, J., Kopp, D. M. and Bledsoe, J. W. (1992). Development of segment- and target-related neuronal activity in the medicinal leech. *J. Exp. Biol.* **170**, 74-92.

Karnovsky, M. J. and Roots, L. (1964). A "direct-coloring" thiocholine method for cholinesterases. *J. Histochem. Cytochem.* **12**, 219-221.

Kuhlman, J. R., Li, C. and Calabrese, R. L. (1985a). FMRF-amide-like substances in the leech. I. Immunocytochemical localization. *J. Neurosci.* **5**, 2301-2309.

Kuhlman, J. R., Li, C. and Calabrese, R. L. (1985b). FMRF-amide-like substances in the leech. II. Bioactivity on the heartbeat system. *J. Neurosci.* **5**, 2310-2317.

Macagno, E. R. (1980). Number and distribution of neurons in leech segmental ganglia. *J. Comp. Neurol.* **15**, 283-302.

Maranto, A. R. and Calabrese, R. L. (1984a). Neural control of the hearts in the leech, *Hirudo medicinalis*. I. Anatomy, electrical coupling, and innervation of the hearts. *J. Comp. Physiol. A* **154**, 367-380.

Maranto, A. R. and Calabrese, R. L. (1984b). Neural control of the hearts in the leech, *Hirudo medicinalis*. II. Myogenic activity and its control by heart neurons. *J. Comp. Physiol. A* **154**, 367-380.

Nicholls, J. G. and Baylor, D. A. (1968). Specific modalities and receptive fields of sensory neurons in CNS of the leech. *J. Neurophysiol.* **31**, 740-756.

Nusbaum, M. P., Blitz, D. M., Swensen, A. M., Wood, D., Marder, E. (2001). The roles of co-transmission in neural network modulation. *Trends Neurosci.* **24**, 146-154.

Sámano, C., Zetina, M. E., Marín, M. A., Cifuentes, F. and Morales, M. A. (2006). Choline acetyl transferase and neuropeptide immunoreactivities are colocalized in somata, but preferentially localized in distinct axon fibers and boutons of cat sympathetic preganglionic neurons. *Synapse* **60**, 295-306.

Sossin, W. S., Sweet-Cordero, A. and Scheller, R. H. (1990). Dale's hypothesis revisited: different neuropeptides derived from a common prohormone are targeted to different processes. *Proc. Natl. Acad. Sci. USA* **87**, 4845-4848.

Thompson, W. J. and Stent, G. S. (1976a). Neuronal control of heartbeat in the medicinal leech. I. Generation of the vascular constriction rhythm by heart motor neurons. *J. Comp. Physiol.* **111**, 261-279.

Thompson, W. J. and Stent, G. S. (1976b). Neuronal control of heartbeat in the medicinal leech. II. Intersegmental coordination of heart motor neuron activity. *J. Comp. Physiol.* **111**, 281-307.

Thompson, W. J. and Stent, G. S. (1976c). Neuronal control of heartbeat in the medicinal leech. III. Synaptic relations of the heart interneurons. *J. Comp. Physiol.* **111**, 309-333.

Vaney, D. I. and Young, H. M. (1988). GABA-like immunoreactivity in NADPH-diaphorase amacrine cells of the rabbit retina. *Brain Res.* **474**, 380-385.

Wallace, B. G. and Gillon, J. W. (1982). Characterization of acetylcholinesterase in individual neurons in the leech central nervous system. *J. Neurosci.* **2**, 1108-1118.

Wenning, A. and Meyer, E. P. (2007). Hemodynamics in the leech: blood flow in two hearts switching between two constriction patterns. *J. Exp. Biol.* **210**, 2627-2636.

Wenning, A., Cymbalyuk, G. S. and Calabrese, R. L. (2004a). Heartbeat control in leeches. I. Constriction pattern and neural modulation of blood pressure in intact animals. *J. Neurophysiol.* **91**, 382-396.

Wenning, A., Hill, A. A. V. and Calabrese, R. L. (2004b). Heartbeat control in leeches. II. Fictive motor pattern. *J. Neurophysiol.* **91**, 397-409.